Defrosting, dark flow features, and dune activity on Mars: Example in Russell crater

Emilie Gardin, Pascal Allemand, Cathy Quantin, Patrick Thollot

Defrosting, dark flow features, and dune activity on Mars: Example in Russell crater

E. Gardin,[1] P. Allemand,[1] C. Quantin,[1] and P. Thollot[1]

[1] Defrosting processes observed on Mars are among the most unusual features described on high-resolution images. A defrosting sequence has been observed near the crest of the megadune located in the Russell crater on new high-resolution images obtained from the HiRISE instrument and on hyperspectral cubes obtained from CRISM instrument, both on board MRO. Hyperspectral images show that frost overlaps the entire megadune in middle winter. This frost is composed mainly of CO_2 and of a small amount of water ice. The deepest ice signatures are mainly located near the crest of the megadune. The defrosting sequence monitored by CRISM reveals spatial heterogeneity and refrosting processes. On the morphological counterpart, the defrosting sequence starts with the development of dark spots, similar to those described in the cryptic regions. After few sols, we observe the emplacement of dark linear flow features that start from the dark spots downward of the main slope of the dune. These linear flow features are 1 to 2 m wide and 50 to 100 m long. They settle on the small rills visible on the frost cover. They are interpreted as avalanches of a mixing of sand, dust, and unstable CO_2 gas released under pressure. The avalanches would be triggered by the eruption of the dark spots. The flux of material transported by the flow features has been estimated to 0.25 to 0.5 m^3 by meter width each year on the megadune. This flux is larger than flux transported by wind. These dark flow features are thus very efficient to transport material on slopes located in frosted areas.

1. Introduction

[2] Among the various active Martian geomorphologic processes, those related to defrosting are the most unusual. These defrosting processes have been revealed by high-resolution surveys over the past years [*Albee et al.*, 1998; *Zuber et al.*, 1998; *Hansen*, 1999; *Kieffer et al.*, 2000; *Thomas et al.*, 2000; *Smith et al.*, 2001; *Piqueux et al.*, 2003; *Titus et al.*, 2003; *Kieffer*, 2007]. Each local winter lead to a seasonal polar cap composed by CO_2 and H_2O ices [*Titus et al.*, 2003; *Bibring et al.*, 2004]. At summer solstice time, the southern Martian pole is covered by a widespread seasonal CO_2 cap, which extends to 50°S of latitude. At the end of the spring, this seasonal cap retreats leading to unusual features, which have been highly documented on Mars Orbiter Camera (MOC) images on board Mars Global Surveyor (MGS) mission [*Malin et al.*, 1992]. The defrosting of the seasonal CO_2 cap leads to dark spots [*Bridges et al.*, 2001], spiders [*Piqueux et al.*, 2003; *Hansen et al.*, 2010],

polygonal structures [*Kossacki and Markiewicz*, 2002], and vents [*Piqueux and Christensen*, 2008].

[3] Dark spots are classically interpreted as dust and sand accumulation around CO_2 emitting geysers, which are driven by solar energy which crosscut the transparent CO_2 frost [*Kieffer et al.*, 2000; *Piqueux et al.*, 2003]. The CO_2 gas produced at the interface between the frost and the bedrock erodes then the substratum along convergent channels and transports the eroded material to the vents, where it is ejected in the atmosphere, and falls down at a short distance from it [*Piqueux et al.*, 2003; *Kieffer et al.*, 2006; *Kieffer*, 2007]. After the defrosting, spider structures are visible in the substratum. These spiders consist in a collection of channels of several meter width which converge toward the point where the vent of the dark spot was. A plurimetric hole is located at the convergence of the channels, at the place of the dark spot.

[4] The high-resolution images, MOC first, and now High Resolution Imaging Science Experiment (HiRISE) [*McEwen*, 2007] on board of Mars Reconnaissance Orbiter (MRO), show these uncommon features further north in the southern hemisphere. Indeed, some south up facing scarps in middle latitudes are partly frosted during the local winter and display a defrosting sequence during the spring time retreat. This is the case of Russell crater (54.6°S and 12.4°E),

[1] Laboratoire de Sciences de la Terre, UMR 5570, Université de Lyon, Université Lyon 1, Ecole Normale Supérieure, CNRS, Lyon, France.

Table 1. HiRISE Images and CRISM Hyperspectral Data Cube in Function of the Solar Longitude, the Martian Seasons of the Southern Hemisphere, and the Resolution of HiRISE Images[a]

Seasons	HiRISE	HiRISE Ls (deg)	Resolution (cm pixel^{-1})	CRISM	CRISM Ls (deg)	Dark Spots (low)	Dark Spots (up)	Dark Flows	Polygons	Dust Devils
				First Year of MRO Acquisition						
Winter	PSP_001440_1255	136.3	50			X				
	PSP_001981_1255	157.7	50	FRT39DF	158	X	X			
	PSP_002337_1255	172.6	25	HRS4006	173	X	X	X		
	PSP_002482_1255	178.9	25	FRT42AA	179	X	X	X		
Spring	PSP_002548_1255	181.8	25	HRS43BC	182	X	X	X		
	PSP_002904_1255	197.9	25				X	X		
	PSP_003326_1255	217.7	25	FRT5339	215					
	PSP_003748_1255	238.4	25							X
	PSP_004038_1255	252.7	25							X
	PSP_004249_1255	263.1	25							X
Summer	PSP_005238_1255	310.3	25							X
	PSP_005383_1255	316.8	25	FRT7F9E	323					X
Autumn	PSP_006873_1255	17.2	50	FRT966B	17					X
	PSP_007018_1255	22.5	25							
	PSP_007229_1255	30.1	50							
				Second Year of MRO Acquisition						
Winter	PSP_009879_1255	122.2	100	FRTC55B	122				X	
	PSP_010090_1255	130.1	100			X			X	
	PSP_010301_1255	138.1	100	FRTCD8E	138	X				
	PSP_010446_1255	143.7	50			X	X			
	PSP_010868_1255	160.6	50			X	X			
Spring	PSP_011580_1255	191.5	50			X	X	X		

[a]High-resolution observation of geomorphologic features are also reported: dark spots (low) for lower part of the megadune, dark spots (up) for upper part of the megadune, dark flows for dark flow features, polygon for polygonal structure and dust devils.

a large crater in the southern hemisphere that exposes a large dune field in its center.

[5] The present paper describes the sequence of active features produced by defrosting on the megadune of Russell crater. We will present first the data set used and the geological context of our observations. We will then expose the defrosting sequence in terms of frost distribution from both Compact Reconnaissance Imaging Spectrometer for Mars (CRISM) data [Murchie et al., 2007] and morphologic features from HiRISE images on board MRO mission. The present study leads to a discussion on both defrosting processes themselves and current transport mechanisms on dunes.

2. Data Set

[6] MRO did a large effort on surveying the defrosting sequences over the Russell megadune with HiRISE and CRISM. HiRISE is a camera which collects images at a resolution ranging from 0.25 to 1 m in a 6 km wide swath [McEwen, 2007]. HiRISE images on the dune field of the Russell crater were acquired at different times during the defrosting period. Some images were acquired only a few Martian days apart (Table 1). We studied 22 available HiRISE images on the Russell crater megadune, which completely covered the first year of HiRISE acquisition and the beginning of the second, from Ls 136° to Ls 191° of the second acquisition year (Table 1). For this study, the 22 HiRISE images were downloaded at full resolution, geoprocessed, and inserted in a Geographic Information System (GIS) in order to compare and measure the changes between each image.

[7] CRISM is the spectral imager on board of MRO that measures the reflectance in the visible and near-infrared wavelengths [Murchie et al., 2007]. In hyperspectral mode,

CRISM collects 544 wavelengths from 0.36 to 3.96 μm in ~10–12 km wide swaths at 18–36 m pixel^{-1} resolution [Murchie et al., 2007]. In the present study, we used only the near-infrared data between 1 and 3.96 μm as diagnostic water and CO_2 ice features occur in the 1–2.5 μm range The data were processed for instrumental effects, converted to I/F and the atmosphere was removed using a ratio with a CRISM scene of Olympus Mons, scaled to the same column density of CO_2. All these processing were done with CRISM Analysis Tool (CAT) v6.5, a public available application [Mustard et al., 2008] based on ENVI software. This software was released by the CRISM team for public to help the data exploitation. We processed the following images: FRT_39DF, HRS_4006, FRT_42AA, HRS_43BC and FRT_5339 that have been acquired from the solar longitude (Ls) 157° to 215°, covering a period from the middle winter to the end of spring (Table 1).

3. Regional Context

[8] The defrosting features have been observed in Russell crater which is a 134 km diameter depression located west of Hellas basin (Figure 1). This crater hosts a 1700 km^2 dune field with an unusual large dune on its northeastern part of the dune field. This megadune, visible on Mars Observer Laser Altimeter (MOLA) data [Zuber et al., 1992], is about 500 m high, 20 km (with 2.5 km for the southwest facing slope) wide and 40 km long. It has been highly studied as its southwest facing scarp displays gullies [Mangold et al., 2003; Reiss and Jaumann, 2003]. They were interpreted as the result of liquid water bearing debris flows during recent climate changes related to Martian obliquity variations [Laskar et al., 2004]. This southwest facing slope is steep with an average slope of about 10°. The
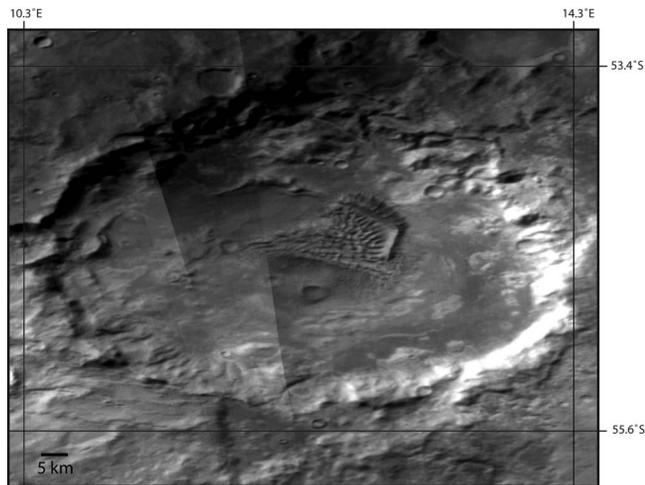
Figure 1. Context of the Russell crater dune field. MOC-WA images show the dune field inside the Russell crater of 150 km diameter. It is located in the northeastern part (near the center) of the crater. The megadune can be seen in the northeastern part of the dune field and is composed by a steeper and southwest facing slope and a gentler and northeast facing slope.

slope is exposed to seasonal frost and we reported in the present study the defrosting sequence on it (Figure 1). The upper part of the southwest facing slope of the megadune is not resolved on MOLA data. However, shadows and luminance variations on HiRISE images suggest that this slope is steeper just under the crest on a high of some tenths of meters. This part corresponds to heads of the gullies. The northeast facing slope of the megadune has an average slope of 2°. This northeast facing slope is reshaped by longitudinal (linear) dunes with a frontal progress toward the northeast.

[9] The megadune can be interpreted as a transverse dune built first by a wind trend coming from the northeast with a northeast facing slope interpreted as the windward slope and a southwest facing slope interpreted as the avalanche slope. After a first phase of building, the large transverse dune has been modified by a bidirectional regime of winds, coming mainly from SW and WNW, which have built the longitudinal dunes.

[10] Over the megadune, many ripples are observed. On the southwest facing slope, the orientation of the ripples is mainly oblique to the crest of the megadune (NNW–SSE). On the northeast facing slope of the megadune, the orientation of the ripples is mainly parallel to the crest of the megadune. The shadow and luminance variations on the HiRISE images give an estimation of the ripple height of about 1.5 m and are typically 5 m apart. On the slipfaces of the longitudinal dunes, many ripples are also observed. The megadune's ripples have the same wavelength than the aeolian ridges, visible during the summer when the dune is defrosted (Figure 4f). These particular ripples look like the Transversal Aeolian Ridges (TARs), observed by [Balme et al., 2008] above many dark Martian dune fields.

[11] Other geologic features are observed over the megadune [Gardin et al., 2009a, 2009b] and their time of occurrence is reported in Table 1. During the cold seasons, polygonal structures, dark spots and dark flow features appear. In the warmer seasons, the defrosting features have

totally disappeared and many dust devils tracks are observed all over the megadune [Verba et al., 2009].

4. Defrosting Sequence From CRISM Data

[12] The defrosting sequence on the Russell crater megadune is recorded by CRISM data (Figure 2) at Ls 158°, 173°, 178°, and 182°. The spectra at these four successive times show several absorption bands diagnostic of CO_2 ice at 1.435 and 2.35 μm. The spectra also show also a weak but noticeable absorption band at 1.50 μm, diagnostic of water ice. The CO_2 ice is the dominant component of the ice cover. The time evolution of the ice cover is illustrated in Figure 3. The maps represent the band depth of the spectra at 1.435 μm. The absorption band is an indicator of the amount and the purity of the CO_2 ice.

[13] The first CRISM observation has been taken during the middle southern winter (Ls 158°) and shows that the CO_2 ice covers the entire megadune. The signature of CO_2 ice is stronger on the lower part of the southwest facing slope of the megadune and on the northeast facing slope of the megadune, at the intersection of the southeast facing slope of the longitudinal dunes and the brink of the megadune (Figure 3a).

[14] After 20 Martian sols, the strongest CO_2 ice signatures are located along the brink of the megadune and at the lower part of the southwest facing slope of the megadune (Figure 3b). The northeast facing slope of the megadune is free of CO_2 ice excepted where longitudinal dunes connect with the megadune brink. At Ls 173°, the CO_2 ice signatures located just under the brink on the south facing scarp are weaker than the surrounding signatures all area show weaker signatures than at Ls 158°.

[15] At the end of winter (Ls 179°), the CO_2 ice signature is generally weaker than at Ls 173°. We inferred that it is due to the defrosting action (Figure 3c). The spatial distribution of the CO_2 ice is unchanged compared to Ls 158° (the southwest facing slope of the megadune just under the brink and again on the southeast facing slipface of the longitudinal dunes of the northeast facing slope of the megadune) just at the junction between the longitudinal dunes and the brink of the megadune.

[16] Three sols after Ls 179°, the most intense signature of CO_2 ice is precisely located at the same place than at Ls 179°. The spatial resolution of the CRISM data cube taken at Ls 182° is twice lower than the one taken at Ls 179° thus with a signal/noise ratio doubled. One should therefore compare signatures from these two cubes with caution. Indeed, the CO_2 ice signature at Ls 182° (Figure 3d) appears more intense than at Ls 179°. This particular observation could indicate (1) the cleaning of ice in which particles could migrate down (2) the darkening of the ice cover, which could become transparent enough to reveal the underlying rocky surface, and (3) the partial refrosting of the inactive dark flows by late CO_2 ice condensation from the atmosphere.

5. Defrosting Sequence From HiRISE Data

[17] The defrosting sequence over the southwest facing slope of the megadune is illustrated on Figure 4. Dark spots appear first on the slope, while it is covered by frost, in the middle of the southern winter (Ls 158°) (Figure 4a). These
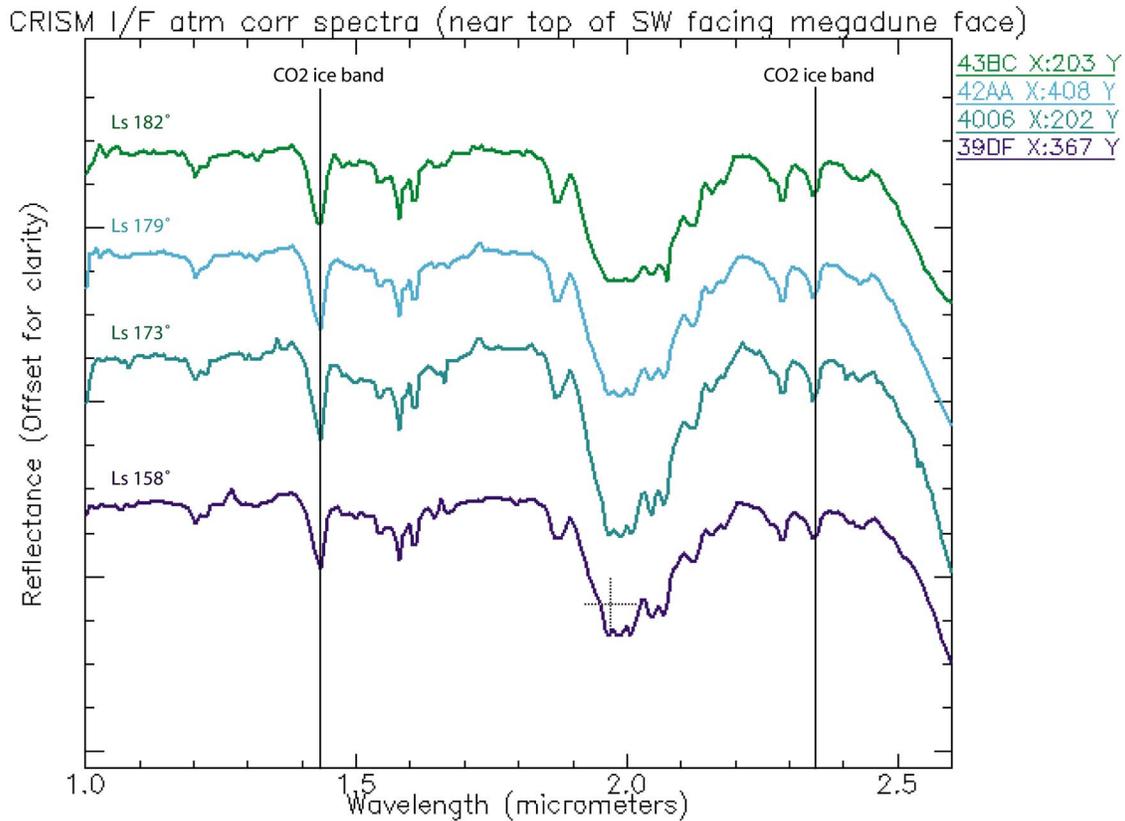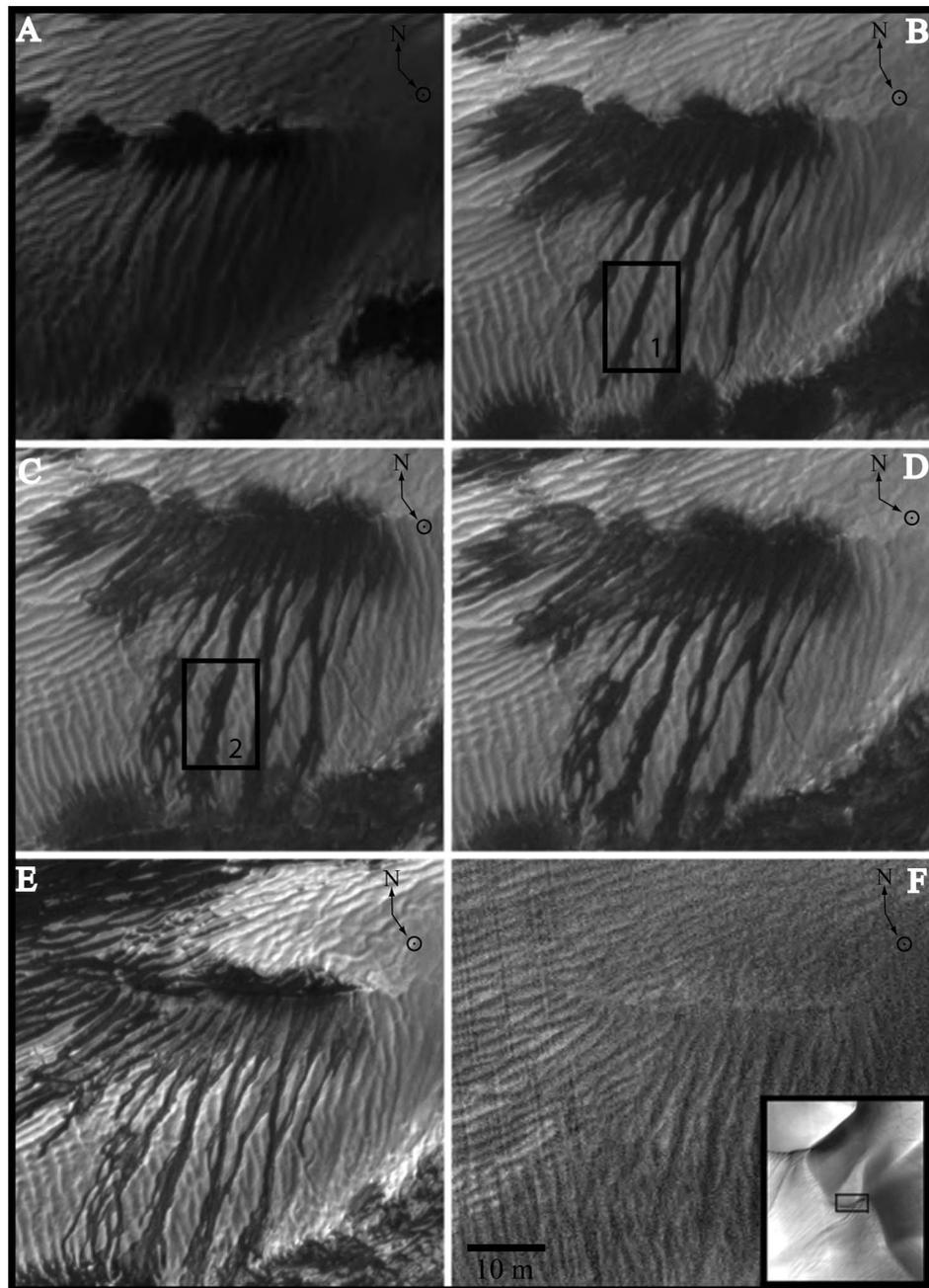
Figure 2. Evolution of the defrosting over the Russell crater megadune observed by CRISM. Four CRISM I/F spectra taken at the base of the megadune at different Ls (offset of 0.5 for clarity). Theses spectra corresponding to Ls 158° until Ls 182° fit the CO_2 ice spectral signature mixed with a small amount of water ice. Vertical bars indicate two main characteristics absorption band of CO_2 ice.

5 m diameter dark spots are located on 100 m long linear bright up facing scarps. The surface of the frost is marked by 5 m large ridges which are oblique to the main slope. This implies that either aeolian ridges are visible by transparency under the frost, or that the frost is thin enough to mold the underlying ridge topography. The diameter of dark spots increases with time. After 15 sols (Ls 173°), the dark spots are coalescent and asymmetric (Figure 4b). They have developed downward and form continuous dark cover along the bright up facing scarps. Dark streaks are visible from the base of dark spots and extend downward the slope at about 100 m. These dark streaks are channelized at the surface. The channels of the dark streaks are sometime diverging and sometime converging. The dark material which marks the spots seems to have flowed between and sometimes over the ridges of about 5 m width. These dark streaks could result from the preferential defrosting between ridges or could be real flows of material from the dark spots over the CO_2 ice. The hypothesis of local defrosting is not supported by both HiRISE and CRISM observations and physics of defrosting. The defrosting should be maximum on the most insulated part of the ridges and thus on their crest or near of it. The defrosting should be asymmetric at the scale of the ridges as the illumination conditions are. Here, the dark streaks are symmetric and located between ridges crests. This is in favor of the flow hypothesis and in the rest of this paper we will call these features "dark flows." The image of the
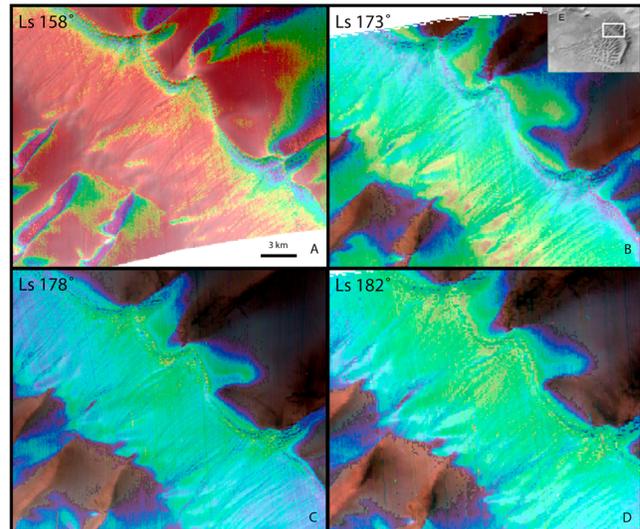

Figure 3. The four maps present the 1.435 μm band depth at different Ls overlapping a color composite (R, 2.5 μm; G, 1.5 μm; B, 1.25 μm). We used the BD1435 criteria from *Pelkey et al.* [2007]. The rainbow color ramp is stretched from 0.1 to 0.3, red color for more CO_2 ice and blue color for few ices. (a) CRISM data FRT39DF (Ls 158°). (b) CRISM data HRS4006 (Ls 173°). (c) CRISM data FRT42AA (Ls 178°). (d) CRISM data HRS43BC (Ls 182°).

Figure 4. Evolution of the defrosting on the southwest facing slope of the megadune. (a) HiRISE image PSP_001981_1225 (Ls 158°). (b) HiRISE image PSP_002337_1225 (Ls 173°). (c) HiRISE image PSP_002482_1225 (Ls 179°). (d) HiRISE image PSP_002548_1225 (Ls 182°). (e) HiRISE image PSP_002904_1225 (198°). (f) HiRISE image PSP_004038_1225 (Ls 252°). The insert in Figure 4f indicates the position of the observation.

Figure 4c has been taken 6 sols after the previous one (Ls 179°). The geometry of the dark spots has not changed. The length and the number of most of the dark flows have increased. They join the other group of dark spots visible at the bottom of the image (in Figure 4). The dark flows are braided at their bases where they divide in small channels always located between the ridges. In more details (black box in the Figures 4b and 4c), the extremity of some dark flows seems to jump above the ridges which are at the frosty surface (Figure 5). This is in favor of an inertial discontinuous flow. The last two images of defrosting (Figures 4d and 4e) have been taken at only 16 Martian sols apart: 4d image in the early spring (Ls 182°) and 4e image in middle spring (Ls 198°). The dark flows are less active than before, in the middle winter. Only few of them have changed in length. In summer, the dune is completely defrosted (Figure 4f). The place of the starting point of dark spots and dark flows, which are visible in the winter frost, is occupied
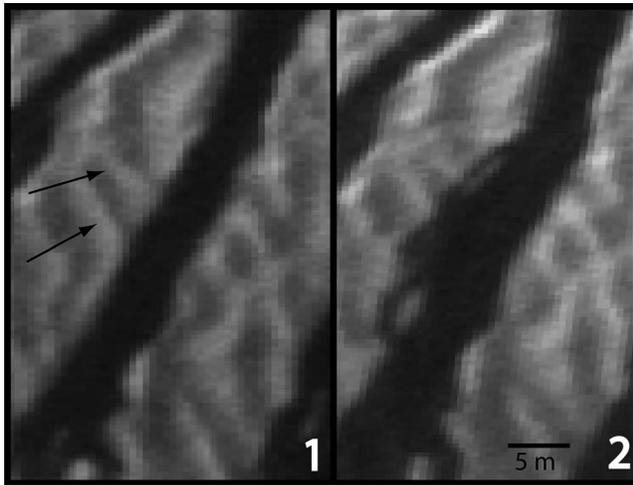
Figure 5. Close-up of Figures 4b and 4c. Here, 1 is taken at Ls 173°, and 2 is taken at Ls 179°. The resolution of the HiRISE images have been degraded for looking the evidence of ripples overpassed.

by a horizontal up facing scarp, which could be more resistant than the surrounding rocks.

[18] The defrosting sequence on the northeast facing slope is briefly illustrated in Figure 6. The dark spots appear in winter and are aligned on bright fractures visible in the frost cover, and mainly perpendicular to the crest of the megadune (Figures 6a and 6b). The size of the dark spots increases with time and they become coalescent along these bright

fractures. No flow features are visible. The aeolian ridges molded by the frost, are perpendicular to the main northeast facing slope and contribute to prevent the development of the dark flow features. On images taken during the Martian summer (Figures 6c and 6d), the defrosted surface displays structures which are quiet similar to the "spiders" described by *Piqueux et al.* [2003]. The position where the dark spots were located, is marked by radial channels which converge toward positive topographies ("bumpy spiders") not observed on the south seasonal polar cap. These small knobs have a diameter of 3 to 5 m. Their height is difficult to estimate because their shadows were not observed probably due to the spherical bumpy shape and the very small height. They are aligned perpendicularly to the crest of the megadune because they follow the bright fractures. Close to the crest, ramified channels are observed with a global elongation aligned along the knob direction ("linear spiders").

[19] The defrosting sequence located on the longitudinal dune slipfaces above the northeast slope of the megadune is illustrated briefly in Figure 7. Numerous and contiguous dark spots appear on the southeast facing slipfaces of a longitudinal dune (Figure 7a) along several alignments perpendicular to the crest of the megadune. These alignments are separated from about 150 m. Dark flow features similar to those described before appear on the Ls 198° HiRISE image (Figure 7b). However, they are smaller than the previous described ones. In summer (Figure 7c), the place occupied by dark spots consists in more or less continuous up facing scarp. Above these scarps, channels converge toward the scarps. These channels would play a
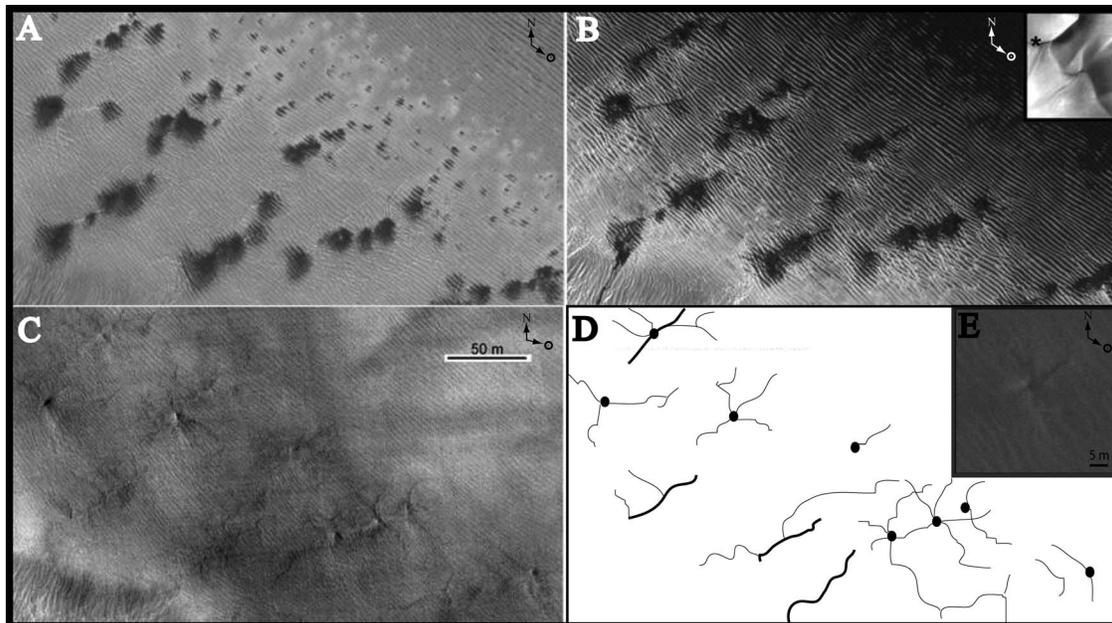
Figure 6. Evolution of defrosting on the northeast facing slope of the megadune, just under the brink. The north and subsolar azimuths are reported for each image. (a) HiRISE image PSP_002482_1225(179°), (b) HiRISE image PSP_002904_1225(198°). (c) HiRISE image PSP_004038_1255(252°). Transversal Aeolian Ridges (TARs) are oriented perpendicular to the main slope of the northeast facing slope. (d) Sketch of Figure 6c showing the geometry of the spiders with central bumps. The black circles symbolize the hill of the bumpy spiders. The widest black curves represent the bright fractures (or linear spiders), where dark spots will appear during the wintertime. They are perpendicular to the crest of the megadune. The small black lines are channels, which converge to the bump (black circle). (e) Close-up of one typical bumpy spider.
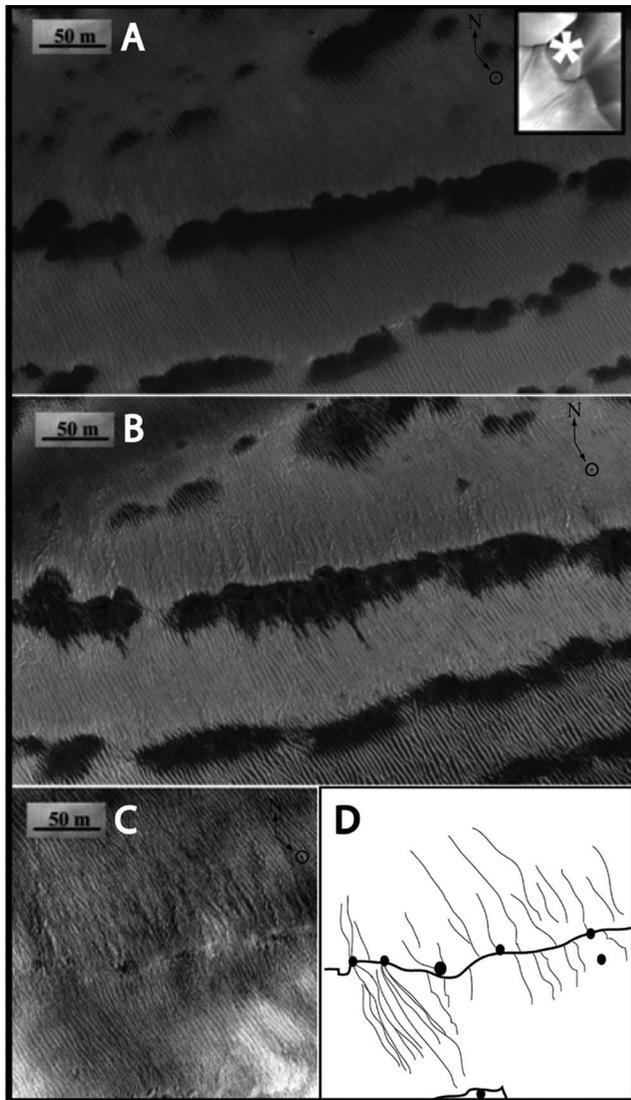
Figure 7. Evolution of defrosting on the slope of a longitudinal dune located on the northeastern side of the megadune. The north and subsolar azimuths are reported for each image. (a) HiRISE image PSP_002337_1225(173°). (b) HiRISE image PSP_002904_1225(198°). (c) HiRISE image PSP_007018_1255(22.5°). (d) Sketch of Figure 7c showing the geometry of the asymmetric spiders. The black circles symbolized the hills of the bumpy spiders. The bold black lines are the up facing scarps above the slip face of the longitudinal (linear) dunes of the northeast facing slope. The thin black lines represent the channels of the asymmetric spiders.

similar role than the channel observed under the seasonal polar cap [*Piqueux and Christensen*, 2008; *Hansen et al.*, 2010] but the overall shape of the structure is asymmetric ("asymmetric spiders").

6. Discussion: Model of Formation of the Seasonal Patterns and Flux of Material on Dune Flanks

[20] On the southwest facing slope of the Russell crater dune field's megadune, the dark spots are mainly located on discontinuous up facing scarps in the upper part and on small hills on the lower part. The reasons of this preferential location can be explained (1) by the thickness of frost which could be thinner on those abrupt zones or mechanically less resistant due to strain stresses or (2) by the CO_2 gas, which could accumulate preferentially in these particular points. As the rheology of CO_2 ice is unknown, it is difficult to test physically these hypotheses. It is however noticeable that the dark spots are localized by heterogeneities at the dune surface. The spiders described on the Russell megadune are not similar to those already described more at the south pole [*Kieffer et al.*, 2000; *Piqueux et al.*, 2003]. Spiders visible under the seasonal south polar cap have a symmetric shape and a hole in their center, just above the vent of the dark spot. In Russell crater, the spiders never have holes in their centers. The channels converge toward positive topographies, which are linear on the major south facing scarp and punctual bumps on north facing scarps. When the slope is not steep, the geometry of spiders is symmetric (Figure 6a) and the center is occupied by a positive bump. When the slope is steep, the channels are developed above the up facing scarps indicating that most flow features comes from above these heterogeneities (Figures 4b–4e). Another class of asymmetric spiders develops near the crest of the megadune. They converge neither to a hole nor to a hill but end at the crest of the megadune (Figure 6b).

[21] Spectral analyses of the CRISM data confirm the presence of CO_2 ice above the megadune (Figure 3) and reveal the time evolution of the ice cover between Ls 158° and 197°. Moreover, a thin amount of water ice has also been detected. This implies that the superficial part of the ice slab is composed by a mixing of CO_2 ice and a small amount of H_2O ice.

[22] Dark flow formation is not a continuous process but seem to be episodic and with a velocity sufficient for dark flow features override small topographies. Three hypotheses can be proposed: (1) the occurrence of the dark flows is triggered by the geyser activity, each geyser emission produces one dark flow, (2) the dark flows are independent from geyser activity and occur when enough particle has accumulated at the base of the dark spot, or (3) the dark flows are active each day when the particle temperature is high enough for the underlying CO_2 ice to sublimate. Some mechanical properties of the dark flows can be assessed by their geometrical characteristics. The dark flows are clearly channelized by the aeolian ridges molding the surface of the frost. Moreover, the contours of the dark flows are bright and net. The width of the aeolian ridges overpassed by dark flows has been measured between 1 and 2 m. If one assumes that the aeolian ridge is between 0.5 to 1.5 m high, the dark flow velocity can be estimated using the principle of energy conservation in mechanics from the equation

$$\frac{1}{2}mv^2 = mgh \tag{1}$$

where m is mass of the dark flow, v is velocity of the dark flow, g is Martian gravity, and h is the height of ridge, overridden by a dark flow. The velocity can thus be approximated by

$$v = \sqrt{2gh} \tag{2}$$

In the studied case, for a height ranging from 0.5 to 2 m and a gravity of 3.7 m s^{-2}, the velocity ranges from 2 to 4 m s^{-1}.

[23] With such a velocity under the Martian low gravity, the material of the dark flows has to be cohesive to maintain a channelized aspect. This cohesion can be due to (1) electrostatic forces between small particles or (2) large diameter of particles.

[24] The amount of material of a single flow feature can be estimated from its geometric characteristics. The length of one dark flow is generally around 50 m to 100 m for a width of around 2 m. The thickness of the dark flows is unknown. *Kieffer et al.* [2006] has shown that the CO_2 frost becomes unstable under or near a frost cover of some centimeters. We assume that the thickness of the dark flows is less than 0.05 m. For instance, if the layer thickness is about 1 cm, the volume of a single flow ranges from 1 to 2 m^3. If we consider that the dark flows occupy 50% of the surface of the upper part of the southwest facing slope of the megadune, the average flux along this slope ranges from 0.25 to 0.5 m^3 by meter width by years. If the density of particles is around 3000 kg m^{-3}, 750 to 1500 kg of particles pass per meter width of dune and by year by this process.

[25] The flux of material transported by wind is difficult to estimate on Mars. However, *Claudin and Andreotti* [2006] propose that dunes are active only during large storms a few times a decade. No evidence of dune displacement has been observed from the first missions indicating that the present-day sand flux driven by wind is very small [*Bourke et al.*, 2004; *Livingstone et al.*, 2007; *Hugenholtz*, 2008; E. Gardin et al., Dune footprints suggest past dune migration and possible geochemical cementation of aeolian dunes on Mars, submitted to Icarus, 2010]. The observation of displacement of material on the dune can argue in favor that the dune is currently eroded at this particular part of the southwest facing slope of the dune.

[26] The occurrence of the dark flows on the track of the gullies present on the megadune of Russell raises the issue of their genetic relationship. First, from a morphological point of view, gullies are linear and symmetric with levees although the dark flows are channelized and anastomosed. Gullies are also 1 order in magnitude larger than the dark flow reported here. Second, there is a difference in age. Gullies are in the first order unchanged morphologies under current conditions whereas the dark flows are seasonal and therefore active processes under current Martian climate. Previous works on gullies activity estimated their age at around 100,000 years [*Reiss and Jaumann*, 2003]. Our observations do not allow us to determine if there is a connection between gullies and dark flows as they emplace in same location.

[27] However our study proposes that the dark flows initiate from the up facing scarps. We interpret the up facing scarps as a more resistant rocky layer that is outcropping on the slope. The presence of such up facing scarps in the upper part of the slope argues for erosionnal processes in opposition to deposition processes at the base of the slope. The gullies formation would be generated by an erosion event [*Costard et al.*, 2002; *Mangold et al.*, 2003; *Reiss and Jaumann*, 2003; *Hugenholtz*, 2008]. This hypothesis is supported by the observation of many alcoves just above the gullies. The unique geological assessment we can propose here is that up facing scarps and gullies require an erosion

area of the upper part of the slope. Future works will be conducted to analyze in more details the relation between gullies and dark flow features.

7. Conclusion

[28] The defrosting of the Russell crater's megadune starts in the middle of winter (Ls 136°) by the development of dark spots, which nucleate on positive topographies of the rocky substratum. These topographies are linear on the southwest facing slope of the megadune or punctual on the northeast facing slope. On the upper part of the southwest facing slope, dark flow features start from the dark spots. Theses dark flow features are channelized between aeolian ridges, which exist over the surface of the megadune. The activity of these dark flow features is episodic and inertial with a minimum velocity of 2 to 4 m s^{-1}. On the images taken during the summer new classes of spiders have been observed, which develop instead of the dark spots. On the northeast facing slope of the megadune the spiders are symmetric with a hill in their center. On the southwest facing slope the spiders are asymmetric with their channels concentrated above the bright up facing scarps indicating that the dark flows came from above up facing scarps. The defrosting history is not a continuous process. CRISM cubes have revealed that refrosting occurs in spring just under the brink of the megadune.

References

Albee, A. L., F. D. Palluconi, and R. E. Arvidson (1998), Mars Global Surveyor Mission: Overview and status, *Science*, 279, 1671–1672, doi:10.1126/science.279.5357.1671.

Balme, M. R., D. Bermann, M. C. Bourke, and J. R. Zimbelman (2008), Transverse Aeolian Ridges (TARs) on Mars, *Geomorphology*, 101, 703–720, doi:10.1016/j.geomorph.2008.03.011.

Bibring, J.-P., et al. (2004), Perennial water ice identified in the south polar cap of Mars, *Nature*, 428, 627–630, doi:10.1038/nature02461.

Bourke, M. C., J. E. Bullard, and O. S. Barnouin-Jha (2004), Aeolian sediment transport pathways and aerodynamics at troughs on Mars, *J. Geophys. Res.*, 109, E07005, doi:10.1029/2003JE002155.

Bridges, N. T., K. E. Herkenhoff, T. N. Titus, and H. H. Kieffer (2001), Ephemeral dark spots associated with Martian gullies, *Lunar Planet. Sci.*, XXXII, Abstract 2126.

Claudin, P., and B. Andreotti (2006), A scaling law for aeolian dunes on Mars, Venus, Earth, and for subaqueous ripples, *Earth Planet. Sci. Lett.*, 252(1–2), 30–44, doi:10.1016/j.epsl.2006.09.004.

Costard, F., F. Forget, N. Mangold, and J. P. Peulvast (2002), Formation of recent Martian debris flows by melting of near-surface ground ice at high obliquity, *Science*, 295, 110–113, doi:10.1126/science.1066698.

Gardin, E., C. Quantin, and P. Allemand (2009a), Defrosting sequence on the Russell megadune, Mars, *Lunar Planet. Sci.*, XL, Abstract 2032.

Gardin, E., C. Quantin, P. Allemand, and P. Thollot (2009b), Dark spot and dark flow development during the seasonal frost retreat on the Russell crater megadune, Mars, paper presented at Third International Workshop on Mars Polar Energy Balance and CO_2 cycle, Abstract 7013, Lunar Planet. Inst., Seattle, Washington, 21–24 July.

Hansen, C. J., N. Thomas, G. Portyankina, A. McEwen, T. Becker, S. Byrne, K. Herkenhoff, H. Kieffer, and M. Mellon (2010), HiRISE observations of gas sublimation-driven activity in Mars' southern polar regions: I. Erosion of the surface, *Icarus*, 205(1), 283–295, doi:10.1016/j.icarus.2009.07.021.

Hansen, G. B. (1999), Control of the radiative behavior of the Martian polar caps by surface CO_2 ice: Evidence from Mars Global Surveyor measurements, *J. Geophys. Res.*, *104*, 16,471–16,486, doi:10.1029/1998JE000626.

Hugenholtz, C. H. (2008), Frosted granular flow: A new hypothesis for mass wasting in Martian gullies, *Icarus*, *197*(1), 65–72, doi:10.1016/j.icarus.2008.04.010.

Kieffer, H. H. (2007), Cold jets in the Martian polar caps, *J. Geophys. Res.*, *112*, E08005, doi:10.1029/2006JE002816.

Kieffer, H. H., T. N. Titus, K. F. Mullins, and P. R. Christensen (2000), Mars south polar spring and summer behavior observed by TES: Seasonal cap evolution controlled by frost grain size, *J. Geophys. Res.*, *105*, 9653–9699, doi:10.1029/1999JE001136.

Kieffer, H. H., P. R. Christensen, and T. N. Titus (2006), CO_2 jets formed by sublimation beneath translucent slab ice in Mars' seasonal south polar ice cap, *Nature*, *442*, 793–796, doi:10.1038/nature04945.

Kossacki, K. J., and W. J. Markiewicz (2002), Martian seasonal CO_2 ice in polygonal troughs in southern polar region: Role of the distribution of subsurface H_2O ice, *Icarus*, *160*(1), 73–85, doi:10.1006/icar.2002.6936.

Laskar, J., A. C. M. Correia, M. Gastineau, F. Joutel, B. Levrard, and P. Robutel (2004), Long term evolution and chaotic diffusion of the insolation quantities of Mars, *Icarus*, *170*(2), 343–364, doi:10.1016/j.icarus.2004.04.005.

Livingstone, I., G. F. S. Wiggs, and C. M. Weaver (2007), Geomorphology of desert sand dunes: A review of recent progress, *Earth Sci. Rev.*, *80*(3–4), 239–257, doi:10.1016/j.earscirev.2006.09.004.

Malin, M. C., G. E. Damielson, A. P. Ingersoll, H. Masursky, J. Veverka, M. A. Ravine, and T. A. Soulanille (1992), Mars Observer Camera, *J. Geophys. Res.*, *97*, 7699–7718, doi:10.1029/92JE00340.

Mangold, N., F. Costard, and F. Forget (2003), Debris flows over sand dunes on Mars: Evidence for liquid water, *J. Geophys. Res.*, *108*(E4), 5027, doi:10.1029/2002JE001958.

McEwen, A. S. (2007), Mars Reconnaissance Orbiter's High Resolution Imaging Science Experiment (HiRISE), *J. Geophys. Res.*, *112*, E05S02, doi:10.1029/2005JE002605.

Murchie, S., et al. (2007), Compact Reconnaissance Imaging Spectrometer for Mars (CRISM) on Mars Reconnaissance Orbiter (MRO), *J. Geophys. Res.*, *112*, E05S03, doi:10.1029/2006JE002682.

Mustard, J. F., et al. (2008), Hydrated silicate minerals on Mars observed by the Mars Reconnaissance Orbiter CRISM instrument, *Nature*, *454*, 305–309, doi:10.1038/nature07097.

Pelkey, S. M., et al. (2007), CRISM multispectral summary products: Parameterizing mineral diversity on Mars from reflectance, *J. Geophys. Res.*, *112*, E08S14, doi:10.1029/2006JE002831.

Piqueux, S., and P. R. Christensen (2008), North and south subice gas flow and venting of the seasonal caps of Mars: A major geomorphological agent, *J. Geophys. Res.*, *113*, E06005, doi:10.1029/2007JE003009.

Piqueux, S., S. Byrne, and M. I. Richardson (2003), Sublimation of Mars' southern seasonal CO_2 ice cap and the formation of spiders, *J. Geophys. Res.*, *108*(E8), 5084, doi:10.1029/2002JE002007.

Reiss, D., and R. Jaumann (2003), Recent debris flows on Mars: Seasonal observations of the Russell crater dune field, *Geophys. Res. Lett.*, *30*(6), 1321, doi:10.1029/2002GL016704.

Smith, D. E., M. T. Zuber, and G. A. Neumann (2001), Seasonal variations of snow depth on Mars, *Science*, *294*, 2141–2146, doi:10.1126/science.1066556.

Thomas, P. C., M. C. Malin, K. S. Edgett, M. H. Carr, W. K. Hartmann, A. P. Ingersoll, P. B. James, L. A. Soderblom, J. Veverka, and R. Sullivan (2000), North–south geological differences between the residual polar caps on Mars, *Nature*, *404*, 161–164, doi:10.1038/35004528.

Titus, T. N., H. H. Kieffer, and P. R. Christensen (2003), Exposed water ice discovered near the south pole of Mars, *Science*, *299*, 1048–1051, doi:10.1126/science.1080497.

Verba, C. A., P. E. Geissler, and the HiRise Team (2009), Comparative anaylsis of Martian dust devil track morphologies in Gusev and Russell craters, *Lunar Planet. Sci.*, *XL*, Abstract 1979.

Zuber, M. T., D. E. Smith, S. C. Solomon, D. O. Muhleman, J. W. Head, J. B. Garvin, J. B. Abshire, and J. L. Bufton (1992), The Mars Observer Laser Altimeter investigation, *J. Geophys. Res.*, *97*, 7781–7797, doi:10.1029/92JE00341.

Zuber, M. T., et al. (1998), Observations of the north polar region of Mars from the Mars Orbiter Laser Altimeter, *Science*, *282*, 2053–2060, doi:10.1126/science.282.5396.2053.

P. Allemand, E. Gardin, C. Quantin, and P. Thollot, Laboratoire de Sciences de la Terre, UMR 5570, Université de Lyon, Université Lyon 1, Ecole Normale Supérieure, CNRS, 2 rue Raphaël Dubois, Lyon, F-69622, Villeurbanne CEDEX, France. (emilie.gardin@ens-lyon.fr)